Contents lists available at ScienceDirect

Carbohydrate Research

Structural analysis of arabinoxylans isolated from ball-milled switchgrass biomass

Koushik Mazumder, William S. York *

Complex Carbohydrate Research Center, University of Georgia, 315 Riverbend Road, Athens, GA 30602, USA

ABSTRACT

Ball-milled alcohol-insoluble residue (AIR) was prepared from switchgrass (*Panicum virgatum* var Alamo) and sequentially extracted with 50 mM ammonium oxalate buffer, 50 mM sodium carbonate, 1 M KOH containing 1% $NaBH_4$, and 4 M KOH containing 1% $NaBH_4$. Arabinoxylan was the most abundant component of the 1 M KOH-extracted fraction, which was treated with endoxylanase to generate oligosaccharides. Gel-permeation chromatography of these oligosaccharides produced three size-homogeneous oligosaccharide fractions with molecular weights of 678, 810, and 1074 Da, corresponding to 5, 6, and 8 pentose units, respectively. Detailed structural analysis of these oligosaccharides was performed using methylation analysis, multiple-step mass spectrometry ($ESIMS^n$), and 1D and 2D NMR spectroscopy. The preferred gas-phase fragmentation pathways were identified for these oligosaccharides, providing extensive sequence information that was completely consistent with structures determined by ab initio NMR analysis. These results demonstrate the high information content of $ESIMS^n$ analysis when applied to cell-wall-derived oligosaccharides and provide standard data that will facilitate the analysis of cell-wall polysaccharide fragments with a sensitivity that is sufficient for the analysis of samples obtained from dissected tissues as well as other small samples.

© 2010 Published by Elsevier Ltd.

1. Introduction

The bioconversion of lignocellulosic biomass to liquid fuels is a key emerging technology for addressing the need for environmentally friendly and sustainable energy sources. Lignocellulosic biomass is a complex composite of many different polysaccharides, proteins, and phenolic polymers derived primarily from the cell walls of grasses and woody plants. Although cellulose, pectin, and hemicellulose are well established as the three main classes of polysaccharides in the cell wall, the exact composition of the cell wall varies considerably both within and between plant species. Considerable attention is currently being focused on switchgrass (*Panicum virgatum*) as a potential source of lignocellulosic biomass in amounts sufficient to support industrial-scale production of biofuels.

Arabinoxylans, which are major components of the cell walls of *P. virgatum* and other grasses, have a backbone consisting of (1→4)-linked β-D-Xylp residues, some of which bear various side chains[1,2] (including α-L-Araf, α-L-Araf-(1→2)-α-L-Araf, and β-D-Xylp-(1→2)-α-L-Araf) at O-2 and/or O-3. Arabinoxylans play a key role in maintaining the structural integrity of the cell walls of these species. Understanding the detailed structure of arabinoxylans in grasses is important in that differences in the molecular features of these hemicellulosic polysaccharides (e.g., degree of branching and spatial arrangement of arabinosyl substituents

along the xylan backbone) have been correlated to altered cell wall properties.[3] This paper describes development and application of analytical methods for the detailed structural analysis of arabinoxylans from grasses, specifically the arabinoxylan of switchgrass, which has enormous potential as a biofuel crop.

Structural characterization of polysaccharides such as arabinoxylan involves identification of their constituent monosaccharide units, the monosaccharide sequence, the linkage position for each glycosidic bond and the presence and location of each branch point. Owing to this inherent complexity, carbohydrate characterization has required the use of diverse analytical methods, among which NMR spectroscopy has played a major role. Recently, highly sensitive, high-throughput methods for the analysis of glycan structure have been developed using combinations of mass spectrometry, HPLC, and digestion with specific *exo-* and *endo-*glycosidases.[4,5]

We now report the characterization of oligosaccharide fragments generated by the enzymatic digestion of aribinoxylans solubilized by alkali extraction of cell walls prepared from switchgrass biomass. The composition and molecular masses of the purified oligosaccharides were determined by GC–MS and MALDI-TOFMS, and detailed structural information was obtained by glycosyl composition analysis, glycosyl linkage analysis, multiple-stage electrospray-ionization mass spectrometry ($ESIMS^n$)[†], and NMR spectroscopy.

---

* Corresponding author. Tel.: +1 706 542 4401; fax: +1 706 542 4412.
 E-mail address: will@ccrc.uga.edu (W.S. York).

† $ESIMS^n$ = multiple-stage electrospray-ionization mass spectrometry, where n = the number of times the isolation–fragmentation cycle has been carried out.

2. Results and discussion

2.1. Isolation of the arabinoxylan oligosaccharides

Cell walls were prepared as an alcohol-insoluble residue (AIR) obtained by organic-solvent extraction of ball-milled switchgrass biomass. AIR was extracted with 1 M KOH to solubilize arabinoxylan, which was treated with endoxylanase to generate a mixture of *xylo*-oligosaccharides.[6,7] The oligosaccharides were fractionated by size-exclusion chromatography on Bio-Gel P-2 (fine) to yield a void fraction and four partially included fractions (Fig. 1).

2.2. Sugar composition analysis of the arabinoxylan oligosacccharides

The monosaccharide compositions of the switchgrass oligosaccharide fractions were analyzed by high-performance anion-exchange chromatography[8] (HPAEC) and gas chromatography–mass spectrometry[9,10] (GC–MS) of monosaccharides or monosaccharide derivatives, respectively, released by acid-catalyzed depolymerization. The resulting arabinose/xylose ratios were 6.7, 2.1, and 3.9 for fractions 2, 3, and 4, respectively. Fraction 5 contained only xylose.

2.3. Methylation analysis of arabinoxylan oligosaccharides

Glycosidic linkage sites for each residue in the oligosaccharides were determined by GC–MS analysis of partially methylated alditol acetate (PMAA) derivatives obtained by per-O-methylation, hydrolysis, reduction, and acetylation of each fraction.[10–12] The results for fractions 2 and 4 (Table 1) are consistent with a backbone consisting of (1→4)-linked xylopyranosyl residues and a single arabinofuranosyl side chain linked to O-3 of an internal xylosyl residue. For fraction 3 (Table 1), the results are also consistent with a (1→4)-linked xylopyranosyl backbone, but with an Ara*f*-(1→2)-Ara*f* side chain.

2.4. Mass spectrometric analysis of the per-O-methylated oligosaccharides

MALDI-TOF spectra of fractions 2, 3, and 4 (Supplementary Figs. S3, S2 and S1) included highly abundant quasi-molecular ions at *m/z* 1097, 833, and 701 indicating the presence of oligosaccharides with 8, 6, and 5 pentosyl residues, respectively.[13] Glycosyl sequences and branching topologies were determined by ESIMS[n] of the per-O-methylated oligosaccharides.[14–16] Methylation of the free hydroxyl groups of oligosaccharides facilitates this analysis by increasing sensitivity and providing mass spectral features that

Table 1
Methylation analysis data (molar ratios) of fractions 2, 3 and 4

| Derivative	Structure[a]	Fraction 4	Fraction 3	Fraction 2
2,3,5-Me$_3$ Ara	T-Ara	0.8	0.8	1.2
2,3,4-Me$_3$ Xyl	T-Xyl	0.8	1.2	1.0
3,5-Me$_2$ Ara	2-Ara	–	0.9	–
2,3-Me$_2$ Xyl	4-Xyl	1.8	2.2	5.4
2-Me Xyl	3,4-Xyl	1.0	1.0	1.1

[a] Residue structure and substituent sites within the oligosaccharide. (T indicates terminal residue.)

are diagnostic for fragmentation events.[17] Each free hydroxyl group that is generated during gas-phase fragmentation of the methylated oligosaccharide can be identified by its characteristic 14-Da mass difference relative to a methylated site. Such unmethylated 'scars' facilitate the interpretation of the resulting MS[n] data, providing key information required for the identification and location of branch points in the glycosyl sequence. The most abundant fragment ions in the ESIMS[n] spectra of the purified, per-O-methylated oligosaccharides were identified as Y and B fragment ions.[17] Due to their high abundance, Y ions were most often selected for secondary fragmentation in order to maximize ion counts for higher order MS[n].

The ESIMS[2] spectrum of per-O-methylated fraction 4 (Fig. 2A), recorded upon fragmentation of the quasimolecular ion at *m/z* 869, includes an abundant Y ion (*m/z* 695) generated by loss of a single pentosyl residue from the precursor ion. Methylation analysis (see above) indicated the presence of a single branched residue, a nonreducing terminal xylosyl residue and a nonreducing terminal arabinosyl residue (see above). Therefore, two isomeric *m/z* 695 ions can exist, one formed by loss of a terminal xylosyl residue and the other formed by loss of a terminal arabinosyl residue. The ESIMS[3] spectrum recorded upon fragmentation of the *m/z* 695 ion is shown in Figure 2B. In this figure, each scar generated by the initial fragmentation giving rise to the precursor ion is indicated by an unrooted arrow, and the scar generated by subsequent fragmentation of the precursor ion is indicated by an arrow crossed by a mass-labeled, dashed line. Fragmentation of the two isomeric precursor ion structures (*m/z* 695) generates two isomeric Y ions (with three pentosyl residues with two scars) at *m/z* 521 and two isomeric B ions (with two pentosyl residues with two scars) at *m/z* 343. The presence of these ions indicates that the penultimate backbone of the oligosaccharide is branched. This conclusion is confirmed by the presence of a Y ion at *m/z* 375 consisting of two pentosyl residues with single scar. The *absence* of a B ion at *m/z* 357 (consisting of two pentosyl residues with single scar) and a Y ion at *m/z* 535 (consisting of three pentosyl residues with
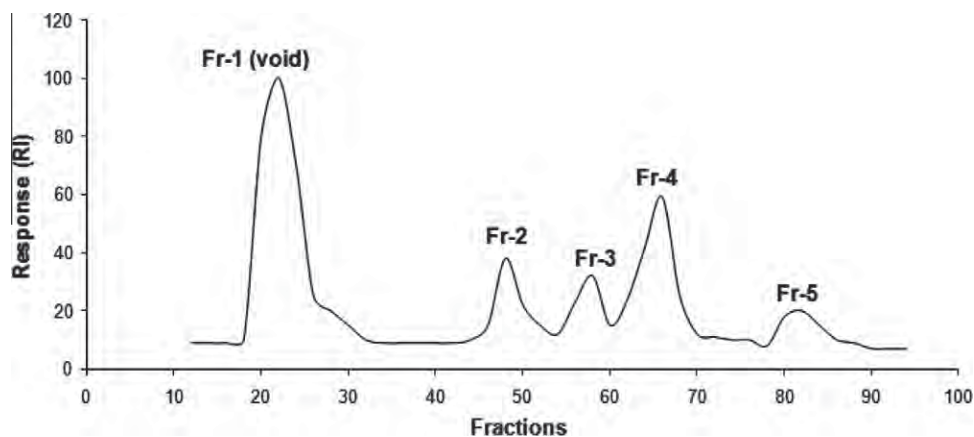
Figure 1. Bio-Gel P-2 size-exclusion chromatography of the endoxylanase-treated 1 M KOH extract.
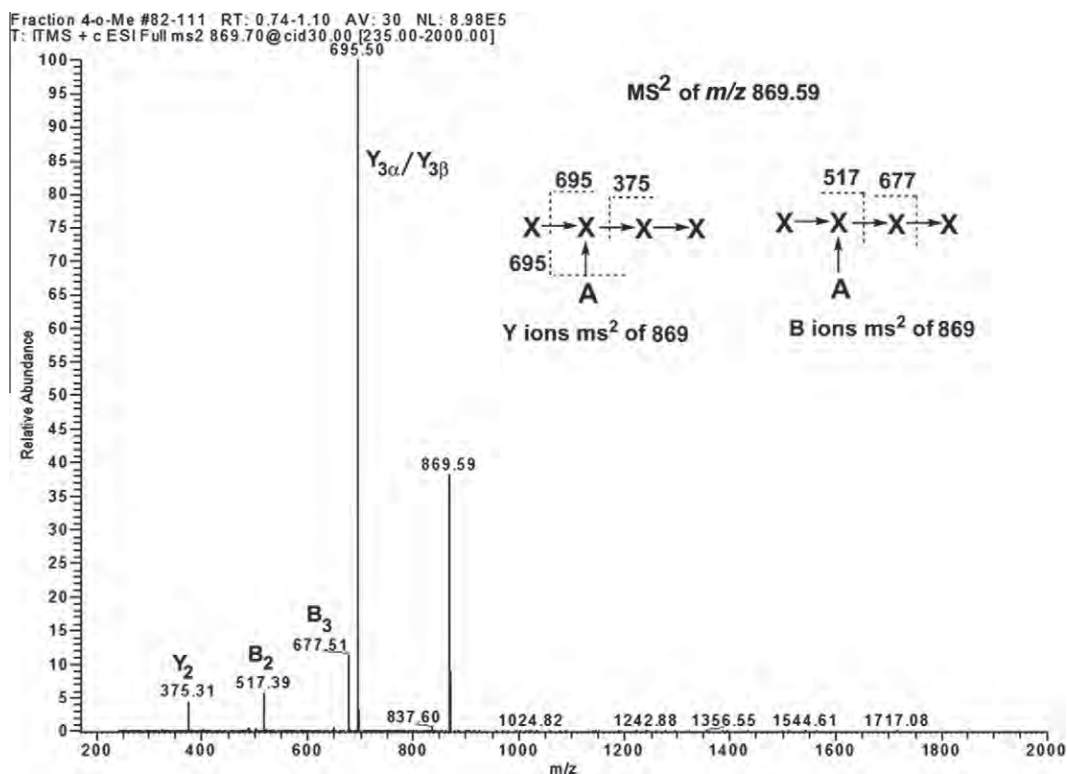
Figure 2A. ESIMS^2 spectrum of per-O-methylated fraction 4.
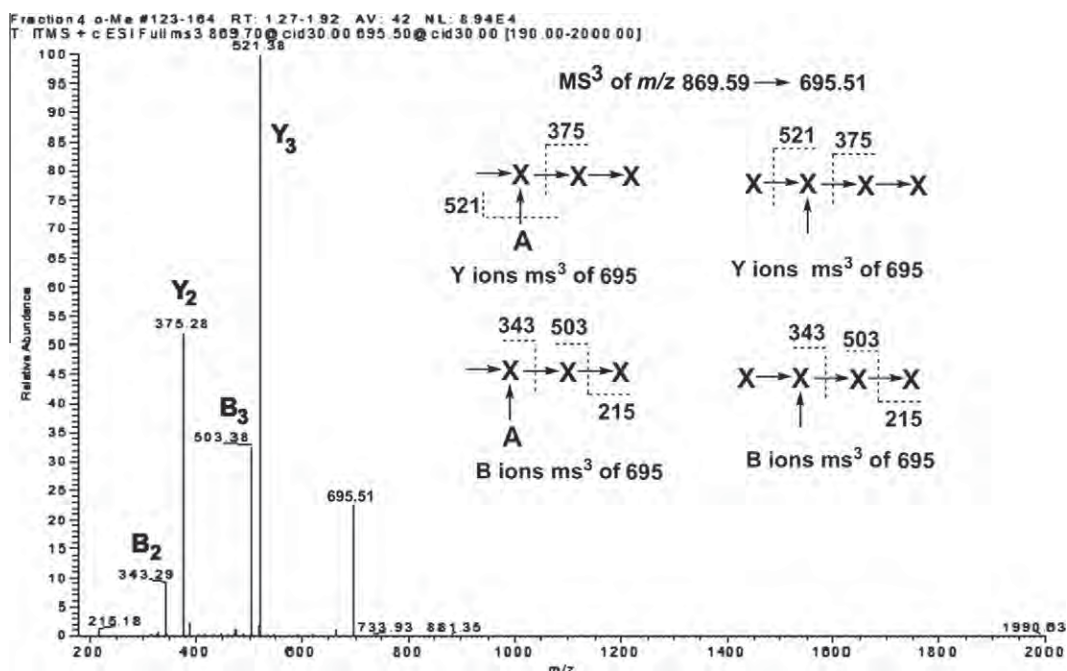
Figure 2B. ESIMS^3 spectrum of per-O-methylated fraction 4 (precursor m/z 695.5).

single scar) indicates that the side chain is not attached to the xylosyl residue adjacent to the reducing end.

The ESIMS^2 spectrum of the per-O-methylated fraction 3 (Fig. 3A) was recorded upon fragmentation of the quasimolecular ion at m/z 1029. This spectrum includes Y ions at m/z 855 and m/z 695, which are formed by the loss of one or two nonreducing pentosyl residues, respectively. Although the m/z 855 ion can form by

loss of either an arabinosyl or a xylosyl residue, the simultaneous presence of both of these ions is consistent with a diarabinosyl side chain, as predicted by methylation analysis (see above). The presence of a Y ion at m/z 375 (two pentosyl residues with single scar) in this spectrum indicates that the backbone residue adjacent to the reducing end does not bear a side chain. As illustrated in Figure 3B, the ESIMS^3 spectrum recorded upon fragmentation of the m/z 855
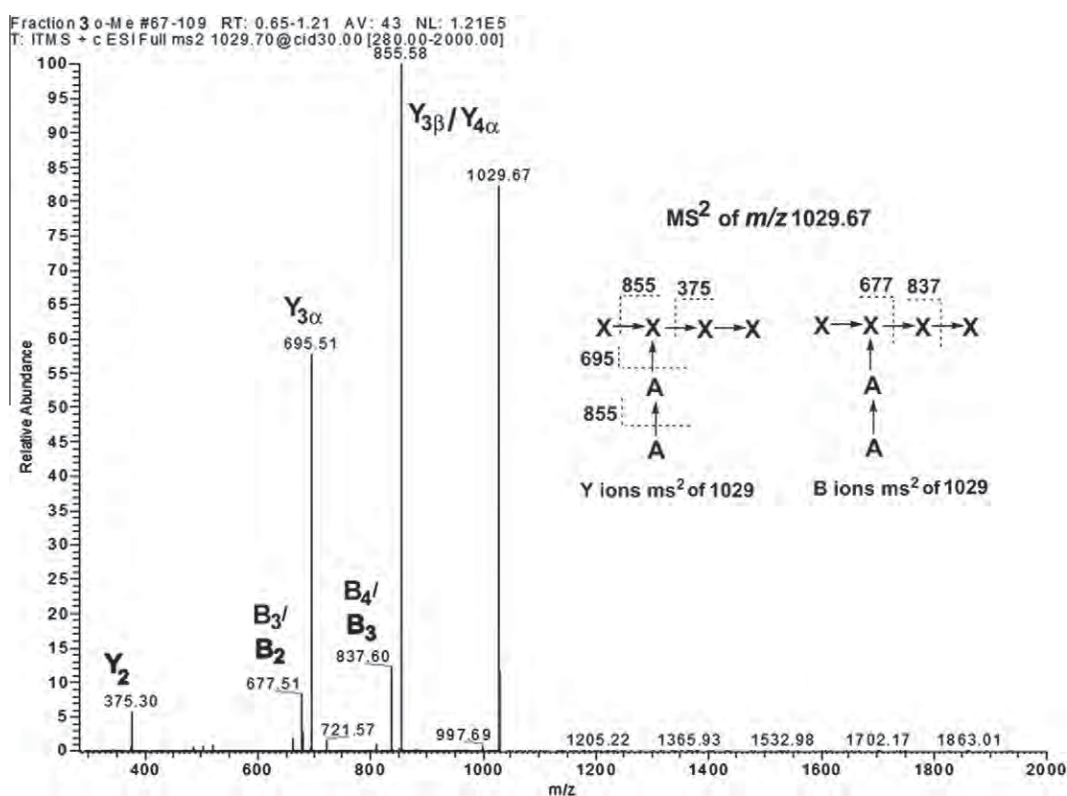
Figure 3A. ESIMS^2 spectrum of the per-O-methylated fraction 3.

ion is consistent with the presence of two isomers of this precursor ion. The presence of a B ion at m/z 503 (two isomers consisting of three pentosyl residues with two scars) and the absence of a B ion at m/z 517 (three pentosyl residues with one scar) indicate that the penultimate residue of the oligosaccharide is branched. Two different pathways (loss of an arabinosyl residue and a xylosyl residue in either order) can give rise to the same Y ion at m/z 681, which has two scars. Only one pathway (loss of the diarabinosyl sidechain) gives rise to the Y ion at m/z 695, which has only one scar. Thus, both the m/z 681 and m/z 695 ions represent a single isomer. The MS^4 spectra (Figs. 3C and D) recorded upon fragmentation of these ions included highly abundant Y ion at m/z 521 (three pentosyl residues with two scars), confirming that the penultimate residue of the oligosaccharide is branched. Together, these data indicate that the penultimate backbone residue of this oligosaccharide bears a dipentosyl side chain.

To maximize sensitivity, only the high-mass regions (m/z >400) of the MS^n spectra of per-O-methylated fraction 2 were recorded. The ESIMS^2 spectrum of the per-O-methylated fraction 2 (Fig. 4A) recorded upon fragmentation of the quasi-molecular ion at m/z 1349 includes a very abundant Y fragment ion at m/z 1175 that was generated by the loss of a single nonreducing terminal pentosyl residue. The ESIMS^3 spectrum (Fig. 4B), recorded upon fragmentation of ion at m/z 1175, includes a very abundant Y ion at m/z 1001, which has two scars, indicating the loss of two nonreducing terminal pentosyl residues by independent events. The presence of this Y ion at m/z 1001 and the *absence* of a Y ion at m/z 1015 (loss of a dipentosyl fragment to form a single scar) indicate that the penultimate residue of the oligosaccharide is branched. The MS^4 spectrum (Fig. 4C) recorded upon fragmentation of the Y ion at m/z 1001 includes a series of Y ions at m/z 855, 695, 535, and 375 that can be formed only by the loss of pentosyl residues to form ions that have a single scar. Together, the glycosyl linkage and MS^n data confirm that the main component of fraction 2 is an octasaccharide

with seven xylosyl residues in the backbone and that the penultimate xylosyl residue in the backbone bears a nonreducing terminal Ara$f$ residue.

2.5. Mass spectrometric analysis of the reduced per-O-methylated oligosaccharides

The most abundant ions in the MS^n spectra of the oligosaccharides were assigned as Y and B ions.[17] However, mass alone cannot distinguish B ions from Z ions with the same monosaccharide composition. The same ambiguity holds for the Y and C ions. It is thus possible that some Z ions were misassigned as B ions and some C ions were misassigned as Y ions. These ambiguities can be resolved by reducing the oligosaccharides prior to methylation, converting the reducing-end residue to an alditol residue. The masses of the Y and Z ions generated by fragmentation of the methylated oligoglycosyl alditols are 16 Da greater than the masses of the corresponding ions generated when reducing oligosaccharides are methylated to form methyl glycosides. The masses of B and C ions are not affected by reduction. Multiple mass spectrometry of the per-O-methylated oligoglycosyl alditols provided spectra (Supplementary Figs. S4–S12) that are comparable to those described above, confirming the B- and Y-ion assignments. That is, the masses of all assigned Y ions increased by 16 Da mass, and the masses of all assigned B ions remained the same. No ions that could be assigned as Z ions or C ions were detected. Thus, B and Y ions are the predominant products formed upon fragmentation of the per-O-methylated xylan oligosaccharides; C and Z ions may be present at very low abundance.

2.6. NMR analysis of the arabinoxylan oligosaccharides

Two-dimensional NMR (i.e., gCOSY and HSQC) experiments were performed to identify and assign resonances for the isolated spin
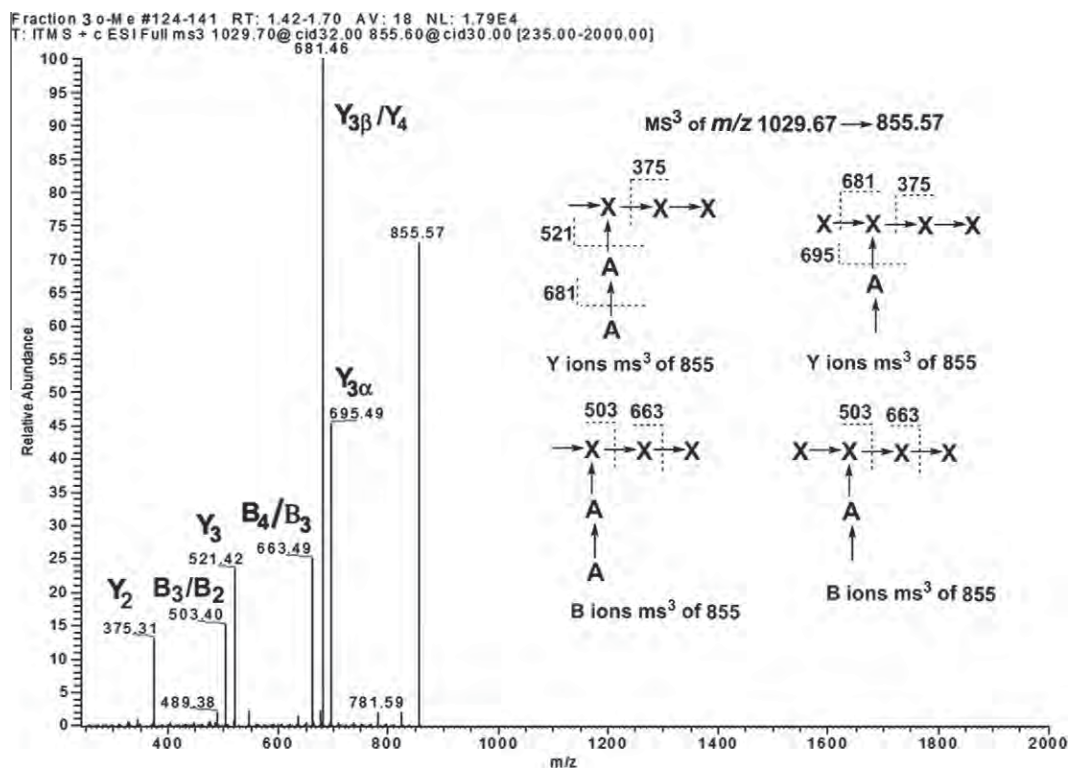
Figure 3B. ESIMS[3] spectrum of the per-O-methylated fraction 3 (precursor m/z 855.6).
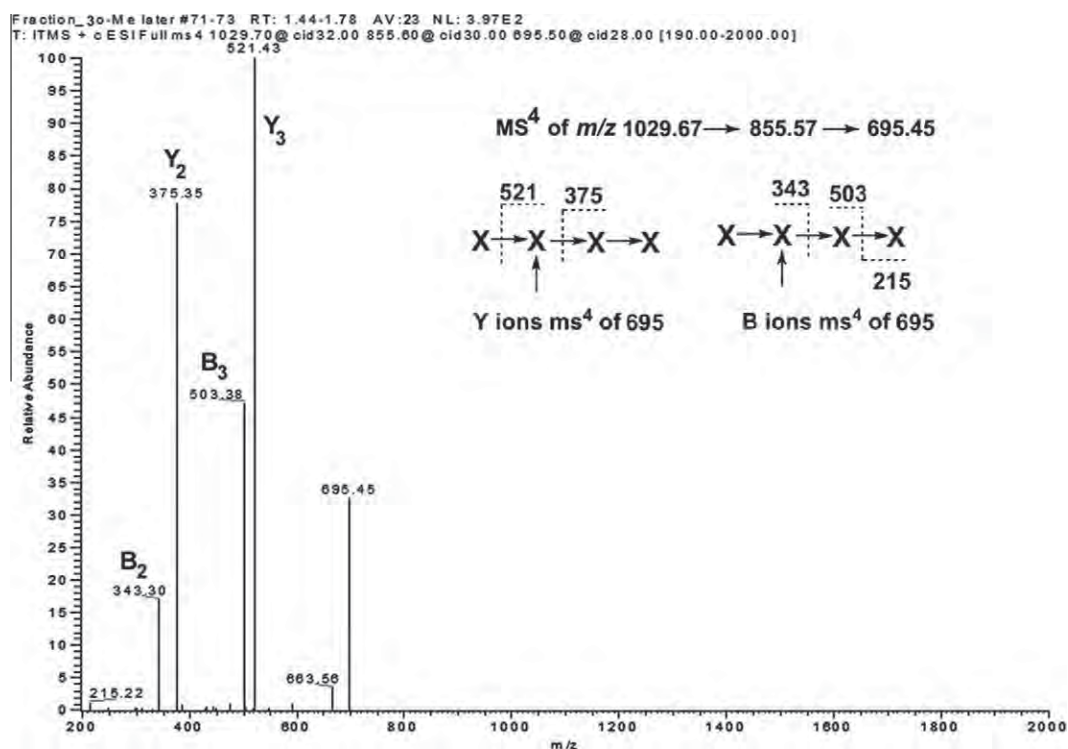

Figure 3C. ESIMS[4] spectrum of the per-O-methylated fraction 3 (precursor m/z 695.5).

system corresponding to each glycosyl residue in the oligosaccharides. Resonance assignments were consistent with published assignments of structurally related oligosaccharides derived from wheat arabinoxylan[18–20] and sorghum glucuronoarabinoxylan.[2] This analysis established the identity, the anomeric configuration and the ring form of each of the constituent glycosyl residues. Analysis of glycosylation shift effects and ROESY spectra provided information regarding glycosyl-linkage sites and residue sequences.

Fractions 2 and 4. The NMR spectra of the structurally homologous oligosaccharides in fractions 2 and 4 contain resonances that
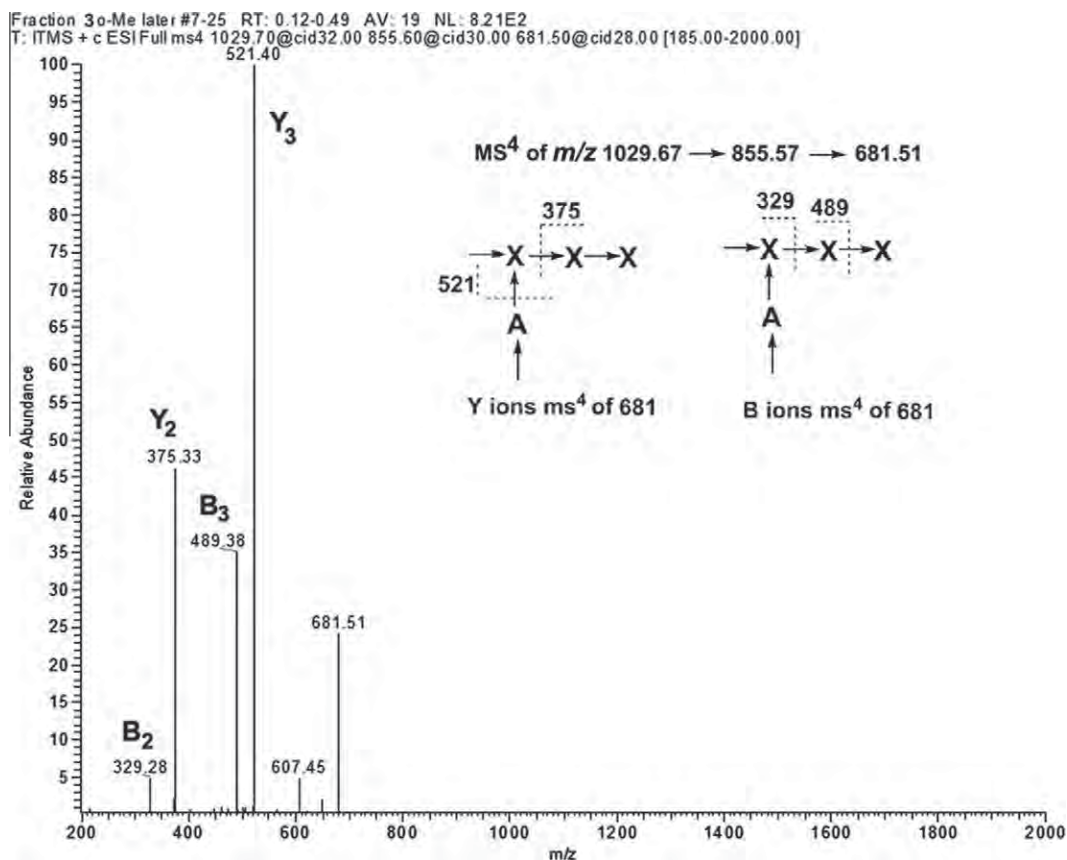
Figure 3D. ESIMS[4] spectrum of the per-O-methylated fraction 3 (precursor m/z 681.5).
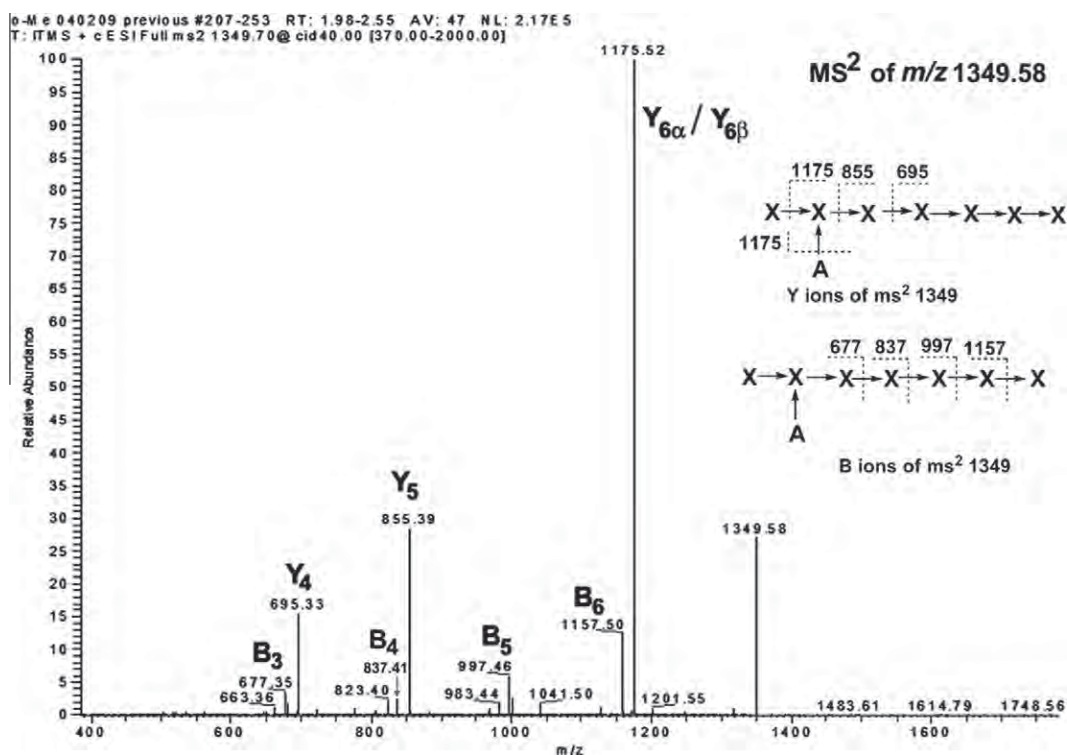

Figure 4A. ESIMS[2] spectrum of the per-O-methylated fraction 2.

are diagnostic for the presence of a single α-L-Araf side chain attached to the penultimate residue of a backbone consisting of (1→4)-linked β-D-Xylp residues (Supplementary Figs. S13 and S14, Tables S1 and S2). NMR assignments for the pentasaccharide
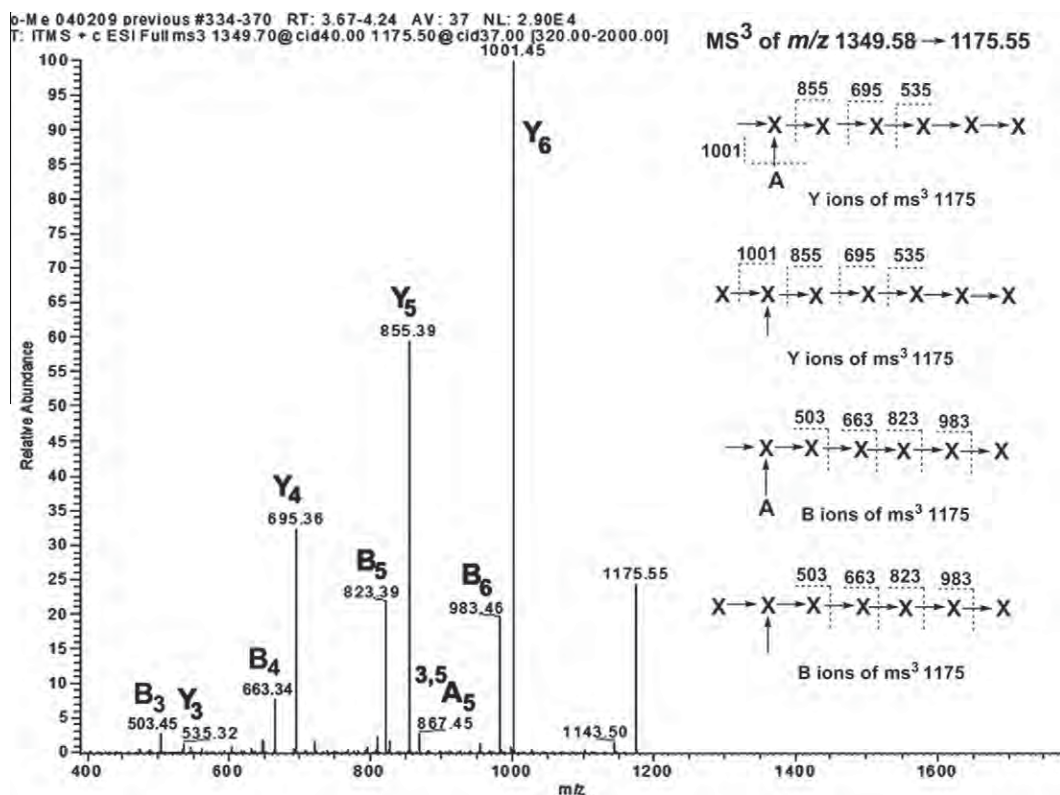
Figure 4B. ESIMS^3 spectrum of the per-O-methylated fraction 2 (precursor m/z 1175.5).

in fraction 4 have been previously reported by Vliegenthart and co-workers.[18] Scalar coupling constants ($^3J_{1,2}$ 8.0 Hz) indicate that, with the exception of α-reducing residues, all xylopyranosyl residues have the β configuration and that the arabinofuranosyl residues have the α configuration ($^3J_{1,2}$ ~1.0 Hz). The ROESY spectrum of fraction 4 (Table 3, Supplementary Figs. S15 and S16) reveals cross peaks between H-1 of β-D-Xylp^n and H-4 of β-D-Xylp^{n-1} residues, together with strong dipolar interactions between H-1 of the α-L-Ara$f$ and H-3 of Xylp^3, confirming the α-L-Ara$f$ side chain is linked to O-3 of the Xylp^3.

Fraction 3. The ^{1}H NMR spectrum (Fig. 5A) included anomeric (H-1) resonances of two α-L-Ara$f$ residues ($^3J_{1,2}$ ~1 Hz) that comprise a diarabinosyl side chain. The structure and molecular location of this side chain can be inferred from the following diagnostic chemical shift effects (Table 2). The H-1, H-2, and C-2 resonances of the 2-linked α-L-Ara$f$ residue ($δ_H$ 5.548, $δ_H$ 4.277, and $δ_C$ 88.6, respectively) are shifted downfield relative to the corresponding resonances of the nonreducing terminal α-L-Ara$f$ residue ($δ_H$ 5.397, $δ_H$ 4.162 and $δ_C$ 81.0). As expected, the presence of the α-L-Ara$f$-(1→2)-α-L-Ara$f$- side chain also shifts the H-1, H-2, H-3, and C-3 resonances ($δ_H$ 4.525, $δ_H$ 3.447, $δ_H$ 3.783, and $δ_C$ 77.9, respectively) of the branched (3,4-linked) β-D-Xylp^3 residue downfield relative to the corresponding resonances of the unbranched (4-linked) β-D-Xylp^2 residue ($δ_H$ 4.483, $δ_H$ 3.288, $δ_H$ 3.586, and $δ_C$ 73.8).

The ROESY spectrum of fraction 3 (Fig. 5B and Table 3) revealed a dipolar interaction between terminal α-L-Ara$f$ H-1 and H-2 of the 2-linked α-L-Ara$f$, confirming the structure of the α-L-Ara$f$-(1→2)-α-L-Ara$f$- side chain. The presence of a cross-peak correlating H-1 of the 2-linked α-L-Ara$f$ with H-3 of Xylp^3 supported the assignment of O-3 of β-D-Xylp^3 as the attachment site for the side chain. A cross peak correlating H-1 of the terminal α-L-Ara$f$ with H-3 of Xylp^3 was also observed. Due to the compelling mass spectral and chemical linkage data described above and the aforementioned cross peaks correlating H-1 of the terminal α-L-Ara$f$ H-1 with H-2 of the 2-linked α-L-Ara$f$ and H-1 of the 2-linked α-L-Ara$f$

with H-3 of Xylp^3, this cross peak was assigned as a 'non-glycosidic' correlation reflecting the dipolar interaction of two nuclei that are separated by seven bonds (included in the intervening 2-linked α-L-Ara$f$ residue). Such 'non-glycosidic' correlations are rare, but can occur when the inter-nuclear distance is small due to a flexible conformation[21,22] and glycan folding. This observation reinforces the need to corroborate structural assignments using orthogonal analytical methods.

The ROE cross peaks between the H-1 of β-D-Xylp^n and H-4 of β-D-Xylp^{n-1} residues in the ROESY spectrum (Fig. 5C and Table 3) confirmed the sequence of glycosidically linked β-D-Xyl$p$ residues. In addition, ROESY cross peaks correlating H-1 of β-D-Xylp^n with H-5$_{eq}$ of β-D-Xylp^{n-1} provide further evidence for the assigned glycosyl sequence. Cross peaks such as these (between the anomeric proton and a proton attached to the carbon that is adjacent to the glycosylation site of the next residue) are not uncommon, although in some cases such cross peaks can lead to incorrect assignment of the glycosylation site. This is not a problem for these xylan oligosaccharides, as the xylosyl residues are in the pyranosyl form, ruling out the possibility of an interglycosidic (1→5)-linkage. NMR analysis of the hexasaccharide in fraction 3 thus provides a complete, independent structural assignment that is consistent with that made using chemical and mass spectral methods.

3. Conclusions

In this study, the primary structures of the major arabinoxylan oligosaccharides obtained by *Trichoderma viride* endo-(1→4)-xylanase treatment of switchgrass arabinoxylan have been determined. ^{1}H NMR, 2D NMR spectroscopy, in combination with monosaccharide analysis, methylation analysis, molecular mass determination (MALDI-TOFMS), and ESIMS analysis showed that the backbone is made up of linear β-D-(1→4)-Xyl$p$ units, with α-L-Ara$f$-(1→ and α-L-Ara$f$-(1→2)-α-L-Ara$f$-(1→ side chains at O-3 of the xylopyranosyl residues.
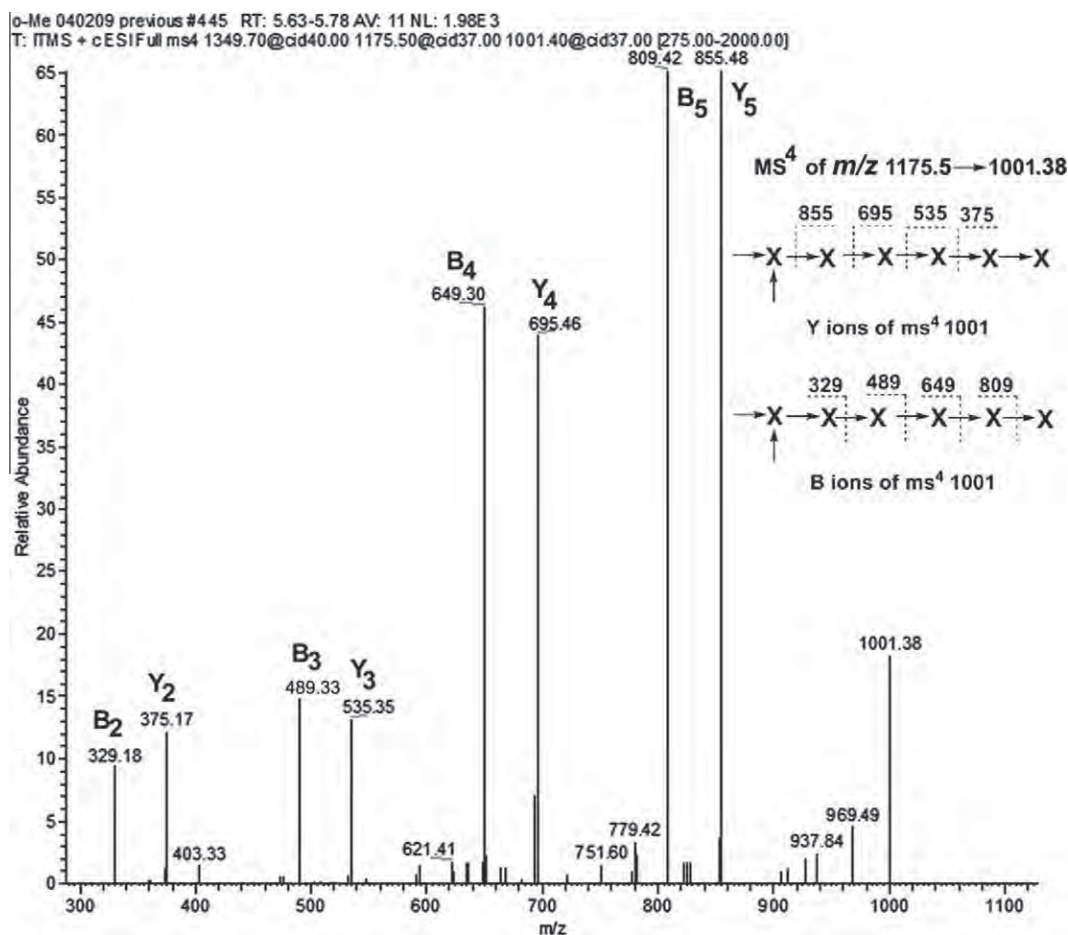
Figure 4C. ESIMS[4] spectrum of the per-O-methylated fraction 2 (precursor *m/z* 1001.4).

We have demonstrated the utility of per-O-methylation followed by ESIMS[n] analysis for characterizing the glycosyl sequences and branching patterns of arabinoxylan oligosaccharides. The data generated by rigorous characterization of arabinoxylan oligosaccharides by a combination of NMR spectroscopy and mass spectrometric analysis can be used to standardize the identification of specific structures in diverse biomass crops. The strength of the mass spectrometric approach described here is its high sensitivity relative to many other analytical techniques such as NMR spectroscopy. This will allow specific arabinoxylan structures to be identified in minute samples that are prepared, for example, by microdissection of plant tissues, providing an insight into the anatomical distribution of these structures and developmental regulation of their synthesis in growing tissues.

4. Experimental

4.1. Isolation of cell walls and extraction of arabinoxylans

Cell walls were prepared as an alcohol-insoluble residue (AIR) of switchgrass (*P. virgatum* var Alamo, BioEnergy Science Center) by ball milling in 80% aq EtOH at 4 °C, 16 h. The residue was washed with acetone and dried under vacuum. The AIR (0.5 g) was sequentially extracted[23] with 35 mL of ammonium oxalate buffer (50 mM), 35 mL of sodium carbonate (50 mM), 35 mL of 1 M KOH, and finally 35 mL of 4 M KOH containing 1% NaBH₄. The 1 M KOH and 4 M KOH extracts were neutralized with glacial HOAc and all the fractions were dialyzed against water.

4.2. Enzymatic treatment of the 1 M KOH extract

The 1 M KOH extract (25 mg) was incubated with endoxylanase (12 units, *T. viride*, Megazyme) in ammonium formate buffer (50 mM, pH 5.0) at 37 °C for 24 h. The enzyme activity was destroyed by heating the reaction mixture for 10 min in a boiling water bath and centrifuged. Oligosaccharides in the supernatant were purified by SEC using Bio-Gel P-2 (fine) column (90 × 1.8 cm) eluted with water and refractive index monitoring.

4.3. Glycosyl composition analysis

The sugar composition of the oligosaccharides was determined by GC–MS of the alditol acetate derivatives[9] and by HPAEC chromatography[8] of underivatized monosaccharides on a CarboPac PA20 column using pulsed amperometric detection.

4.4. Methylation analysis of the oligosaccharides

Oligosaccharides were methylated as described by Ciucanu and Kerek.[11] Lyophilized oligosaccharides (~1 mg) were dissolved in dry DMSO (0.2 mL) and adding a freshly prepared NaOH slurry in dry DMSO (0.5 mL). The reaction mixture was allowed to stand at room temperature for 15 min. Iodomethane (MeI, 0.5 mL) was added, and the samples were stirred at room temperature for 30 min. Samples were exposed to a stream of dry nitrogen for ~10 min to remove excess MeI. The samples were partitioned between 2 mL of water and 2 mL of chloroform. The organic layer was collected, washed twice

Table 2
^{1}H and ^{13}C signals of the hexasaccharide isolated from fraction 3

Sugar residues	H-1/C-1	H-2/C-2	H-3/C-3	H-4/C-4	H-5$_{eq}$/C-5	H-5$_{ax}$/C-5
T-α-L-Araf	5.397/107.9	4.162/81.0	3.912/77.0	4.304/84.9	3.818/61.1	3.724/61.4
2-α-L-Araf	5.548/106.7	4.277/88.6	4.077/75.7	4.304/84.3	3.818/61.1	3.724/61.4
β-D-Xylp^4	4.448/101.6	3.253/73.2	3.432/75.9	3.606/69.2	3.947/65.2	3.316/65.2
β-D-Xylp^3	4.525/101.6	3.447/73.3	3.783/77.9	3.859/73.9	4.152/63.3	3.428/63.3
β-D-Xylp^{2β}	4.483/101.6	3.288/73.0	3.586/73.8	3.827/76.5	4.142/63.3	3.411/63.3
β-D-Xylp^{2α}	4.480	3.296				
β-D-Xylp^1	4.596/96.6	3.243/74.2	3.547/73.8	3.797 /76.5	4.072/63.3	3.389/63.3
α-D-Xylp^1	5.191/91.9	3.558/71.5	3.736/71.2	3.806/76.5	3.812/59.3	3.742/59.3

Starting with the xylopyranosyl residues at reducing end (denoted α-D-Xyl^1 and β-D-Xyl^1) the order of nonreducing xylopyranosyl residues is β-D-Xyl^2, β-D-Xyl^3, β-D-Xyl^4. The β-D-Xyl^{2α} and β-D-Xyl^{2β} residues are distinguishable by virtue of their attachment to reducing α-D-Xyl^1 and β-D-Xyl^1 residues, respectively (anomerisation effect). The 2-α-L-Araf residue is linked to O-3 of β-D-Xyl^3, and the T-α-L-Araf residue is linked to O-2 of the 2-α-L-Araf residue.

Table 3
ROE connectivities of the sugar residues Fraction 3 and 4

Fraction	Residue	δ$_H$	Residue	δ$_H$	ROE connectivity
Fraction 4	T-Ara H-1	5.395	T-Ara H-2	4.159	1,2 Intra-ring correlation
	T-Ara H-1	5.395	T-Ara H-3	3.905	1,3 Intra-ring correlation
	T-Ara H-1	5.395	Xyl^3 H-3	3.753	α-L-Araf-(1→3)-β-D-Xylp^3 linkage
	Xyl^4 H-1	4.443	Xyl^4 H-5$_{ax}$	3.287	1,5 Intra-ring correlation
	Xyl^4 H-1	4.443	Xyl^4 H-3	3.416	1,3 Intra-ring correlation
	Xyl^4 H-1	4.443	Xyl^3 H-4	3.835	β-D-Xylp^4-(1→4)-β-D-Xylp^3 linkage
	Xyl^4 H-1	4.443	Xyl^3 H-5$_{eq}$	4.118	non-bonded inter-glycosidic correlation
	Xyl^2 H-1	4.475	Xyl^2 H-5$_{ax}$	3.383	1,5 Intra-ring correlation
	Xyl^2 H-1	4.475	Xyl^2 H-3	3.555	1,3 Intra-ring correlation
	Xyl^2 H-1	4.475	β-Xyl^1 H-4	3.782	β-D-Xylp^2-(1→4)-β-D-Xylp^1 linkage
	Xyl^2 H-1	4.475	β-Xyl^1 H-5$_{eq}$	4.058	non-bonded inter-glycosidic correlation
	Xyl^3 H-1	4.515	Xyl^3 H-5$_{ax}$	3.408	1,5 Intra-ring correlation
	Xyl^3 H-1	4.515	Xyl^3 H-3	3.753	1,3 Intra-ring correlation
	Xyl^3 H-1	4.515	Xyl^2 H-4	3.801	β-D-Xylp^3-(1→4)-β-D-Xylp^2 linkage
	Xyl^3 H-1	4.515	Xyl^2 H-5$_{eq}$	4.102	non-bonded inter-glycosidic correlation
Fraction 3	T-Ara H-1	5.397	T-Ara H-2	4.162	1,2 Intra-ring correlation
	T-Ara H-1	5.397	T-Ara H-3	3.912	1,3 Intra-ring correlation
	T-Ara H-1	5.397	2-Ara H-2	4.277	α-L-Araf-(1→2)-α-L-Araf-(1→ linkage
	T-Ara H-1	5.397	Xyl^3 H-3	3.783	T-Ara H-1 to Xylp^3 H-3 (non-glycosidic)
	2-Ara H-1	5.548	2-Ara H-2	4.277	1,2 Intra-ring correlation
	2-Ara H-1	5.548	2-Ara H-3	4.077	1,3 Intra-ring correlation
	2-Ara H-1	5.548	Xyl^3 H-3	3.783	→2)-α-L-Araf-(1→3)-β-D-Xylp^3 linkage
	Xyl^4 H-1	4.448	Xyl^4 H-5$_{ax}$	3.316	1,5 Intra-ring correlation
	Xyl^4 H-1	4.448	Xyl^4 H-3	3.432	1,3 Intra-ring correlation
	Xyl^4 H-1	4.448	Xyl^3 H-4	3.859	β-D-Xylp^4-(1→4)-β-D-Xylp^3 linkage
	Xyl^4 H-1	4.448	Xyl^3 H-5$_{eq}$	4.152	non-bonded inter-glycosidic correlation
	Xyl^2 H-1	4.483	Xyl^2 H-5$_{ax}$	3.411	1,5 Intra-ring correlation
	Xyl^2 H-1	4.483	Xyl^2 H-3	3.586	1,3 Intra-ring correlation
	Xyl^2 H-1	4.483	β-Xyl^1 H-4	3.797	β-D-Xylp^2-(1→4)-β-D-Xylp^1 linkage
	Xyl^2 H-1	4.483	β-Xyl^1 H-5$_{eq}$	4.072	non-bonded inter-glycosidic correlation
	Xyl^3 H-1	4.525	Xyl^3 H-5$_{ax}$	3.428	1,5 Intra-ring correlation
	Xyl^3 H-1	4.525	Xyl^3 H-3	3.783	1,3 Intra-ring correlation
	Xyl^3 H-1	4.525	Xyl^2 H-4	3.827	β-D-Xylp^3-(1→4)-β-D-Xylp^2 linkage
	Xyl^3 H-1	4.525	Xyl^2 H-5$_{eq}$	4.142	non-bonded inter-glycosidic correlation

The arabinofuranosyl residue linked to the O-3 of β-D-Xylp^3 is denoted as 2-Ara; the terminal arabinofuranosyl residue linked to O-2 of 2-Ara residue is denoted as T-Ara. Starting with the reducing xylopyranosyl residues (denoted Xyl^1), the order of nonreducing xylopyranosyl residues is Xyl^2, Xyl^3, and Xyl^4.

with deionized water, and dried. The dried samples were redissolved in MeOH, and stored at −20 °C until used.

4.5. Preparation of the partially methylated alditol acetate derivatives

The methylated oligosaccharides (∼200 μg) were hydrolyzed with 2 N TFA, 120 °C for 2 h .The hydrolyzed material was reduced with NaBD$_4$ and acetylated with 1:1 acetic anhydride–TFA at 50 °C for 20 min to generate partially methylated alditol acetates (PMAAs).

4.6. GC–MS analysis

Derivatized monosaccharides were analyzed with a Hewlett–Packard chromatograph (5890) coupled to a mass spectrometer. The sample (1 μL) was introduced in the splitless injection mode onto an SP 2330 (30 m × 0.25 mm, 0.25 μm film thickness, Supelco) column using helium as carrier gas. The PMAA derivatives were separated using the following temperature gradient: 80 °C for 2 min, 80–170 °C at 30 °C/min, 170–240 °C at 4 °C/min, 240 °C held for 20 min. Samples were ionized by electron impact at 70 eV.

4.7. Preparation of the reduced per-O-methylated oligosaccharides

The oligosaccharides (∼500 μg) were reduced with 250 μL of 1 M sodium borohydride in 1 M ammonium hydroxide at room temperature for 16 h. The reaction mixture was neutralized with glacial HOAc. The excess glacial HOAc was evaporated with stream of N$_2$, followed by multiple evaporations with 1% HOAc in MeOH
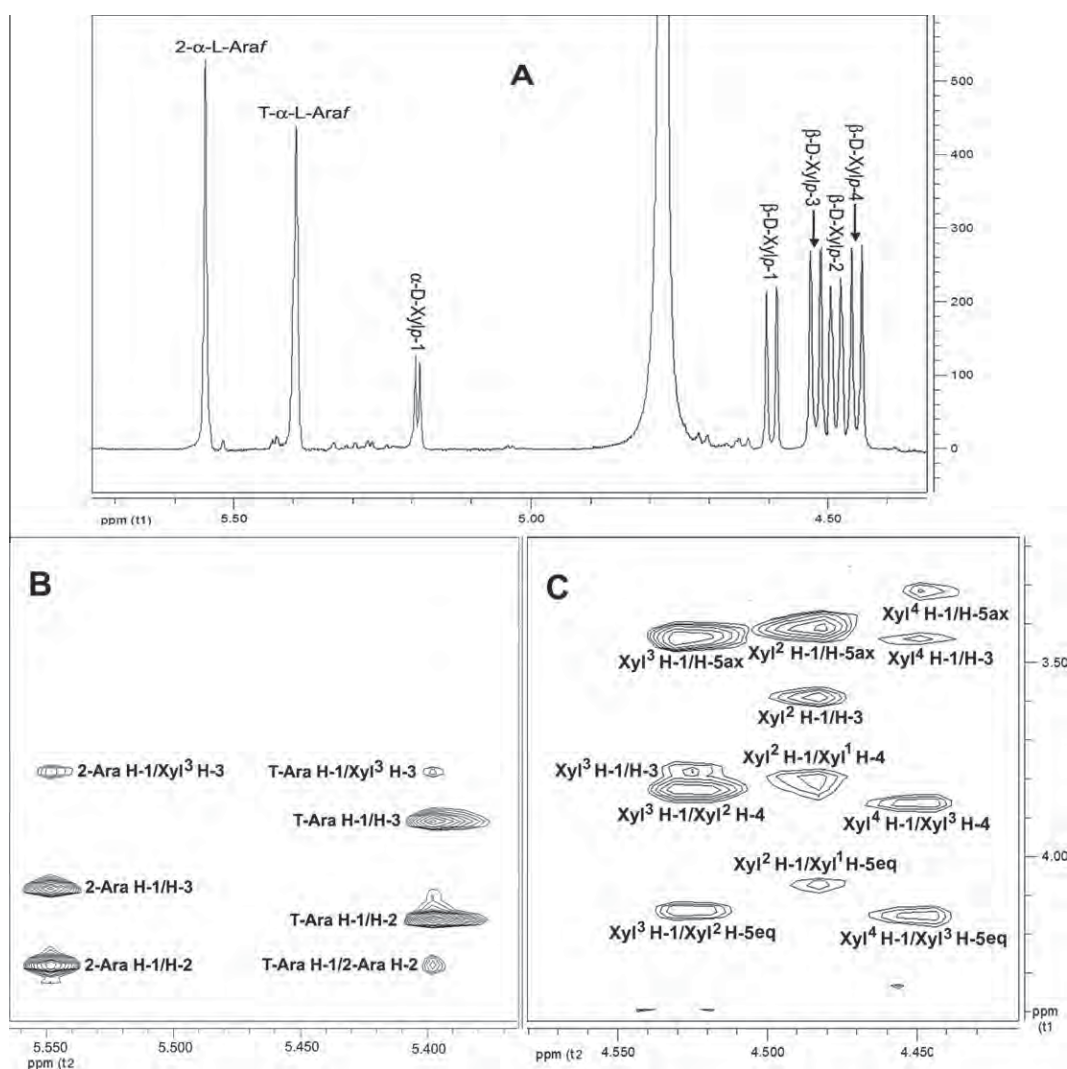
Figure 5. A. ^{1}H NMR spectrum of fraction 3 (anomeric region), B. ROESY spectrum of fraction 3 (arabinosyl residues), C. ROESY spectrum of fraction 3 (xylosyl residues).

(v/v) and a final evaporation with anhyd MeOH. The reduced oligosaccharides were methylated as mentioned above (Section 4.4) to generate reduced per-O-methylated oligosaccharides.

4.8. Mass spectrometric analysis

4.8.1. MALDI-TOFMS

Positive ion MALDI-TOF mass spectra were recorded using an applied biosystems Voyager-DE biospectrometry workstation. Aqueous samples (1 μL of a mg/mL solution) were mixed with an equal volume of matrix solution (0.1 M 2,5-dihydroxybenzoic acid and 0.03 M 1-hydroxyisoquinoline in aq 50% MeCN) and dried on a MALDI target plate. Typically, spectra from 200 laser shots were summed to generate a mass spectrum.

4.8.2. ESI mass spectrometry

The multiple-stage ESI mass spectra were recorded in a Thermo scientific LTQ XL ion-trap mass spectrometer. Ultrapure helium was introduced as the buffer/collision gas, and dry NF grade N_2 was used for sample nebulization. Per-O-methylated and reduced per-O-methylated oligosaccharides in MeOH were diluted with 50% MeCN–H_2O containing 0.1% TFA. Samples were infused through a fused silica capillary (150 μm i.d. × 363 μm o.d. × ∼60 cm, Thermo Finnigan, USA) into the source at flow rate of 3 μL/min using

the syringe pump provided with the instrument. The electrospray source was operated at a voltage of 5.0 kV, and the capillary heater was set to 275 °C. For the most MS^n spectra, the initial collision energies were set to 30 V, though the energies were varied for optimal transmission of the ions into the next stage of analysis. All the experiments were performed in the positive-ion mode.

4.9. NMR spectroscopy

Oligosaccharides (∼3 mg) were dissolved in D_2O (0.5 mL, 99.9%; Cambridge Isotope Laboratories). ^{1}H NMR spectra were recorded with Varian Inova NMR spectrometer operating at 500 MHz and with a sample temperature of 298 K. All two-dimensional spectra were recorded using standard Varian pulse programs. Chemical shifts were measured relative to an internal standard of acetone (δ_H 2.225 ppm, δ_C 30.4 ppm).

Supplementary data

Supplementary data associated with this article can be found, in the online version, at doi:10.1016/j.carres.2010.07.034.

References

1. Ebringerova, A. *Macromol. Symp.* **2006**, *232*, 1–12.
2. Verbruggen, M. A.; Spronk, B. A.; Schols, H. A.; Beldman, G.; Voragen, A. G. J.; Thomas, J. R.; Kamerling, J. P.; Vligenthart, J. F. G. *Carbohydr. Res.* **1998**, *306*, 265–274.
3. Izydorczyk, M. S.; Biliaderis, C. G. *Carbohydr. Polym.* **1995**, *28*, 33–48.
4. Sutton, C. W.; O'Neill, J. A.; Cottrell, J. S. *Anal. Biochem.* **1994**, *218*, 34–46.
5. O'Neill, R. A. *J. Chromatogr., A.* **1996**, *720*, 201–215.
6. Pena, M. J.; Zhong, R.; Zhou, G. K.; Richardson, E. A.; O'Neill, M. A.; Darvill, A. G.; York, W. S.; Ye, Z. H. *Plant Cell.* **2007**, *19*, 549–563.
7. Izydorczyk, M. S.; Biliaderis, C. G. *Carbohydr. Polym.* **1994**, *24*, 61–71.
8. Hardy, M. R.; Townsend, R. R. *Methods Enzymol.* **1994**, *230*, 208–225.
9. Fox, A.; Morgan, S. L.; Gilbart, J. In *Analysis of Carbohydrates by GLC and MS*; Biermann, C. J., McGinnis, G. D., Eds.; CRC Press: Boca Raton, FL, 1989; pp 87–117.
10. Carpita, N. C.; Shea, E. M. In *Analysis of Carbohydrates by GLC and MS*; Biermann, C. J., McGinnis, G. D., Eds.; CRC Press: Boca Raton, FL, 1989; pp 157–216.
11. Ciucanu, I.; Kerek, F. *Carbohydr. Res.* **1984**, *131*, 209–217.
12. Sweet, D. P.; Shapiro, R. H.; Albersheim, P. *Carbohydr. Res.* **1975**, *40*, 217–225.
13. Fernandez, L. E. M.; Obel, N.; Scheller, H. V.; Roepstorff, P. *J. Mass Spectrom.* **2003**, *38*, 427–437.
14. Weiskopf, A. S.; Vouros, P.; Harvey, D. J. *Rapid Commun. Mass Spectrom.* **1997**, *11*, 1493–1504.
15. Sheeley, D. M.; Reinhold, V. N. *Anal. Chem.* **1998**, *70*, 3053–3059.
16. Fernandez, L. E. M.; Obel, N.; Scheller, H. V.; Roepstorff, P. *Carbohydr. Res.* **2004**, *339*, 655–664.
17. Domon, B.; Costello, C. E. *Glycoconjugate J.* **1988**, *5*, 397–409.
18. Hoffmann, R. A.; Leeflang, B. R.; Barse, M. M. J. de; Kamerling, J. P.; Vliegenthart, J. F. G. *Carbohydr. Res.* **1991**, *221*, 63–81.
19. Hoffmann, R. A.; Roza, M.; Maat, J.; Kamerling, J. P.; Vliegenthart, J. F. G. *Carbohydr. Polym.* **1991**, *15*, 415–430.
20. Hoffmann, R. A.; Geijtenbeek, T.; Kamerling, J. P.; Vliegenthart, J. F. G. *Carbohydr. Res.* **1992**, *223*, 19–44.
21. Dervilly, G.; Saulnier, L.; Roger, P.; Thibault, J. F. *J. Agric. Food Chem.* **2000**, *48*, 270–278.
22. Picout, D. R.; Ross-Murphy, S. B. *Carbohydr. Res.* **2002**, *337*, 1781–1784.
23. Selvendran, R. R.; O'Neill, M. A.. In *Methods of Biochemical Analysis*; Glick, D., Ed.; John Wiley & Sons: New York, 1987; Vol. 32, pp 25–152.